3D PROCESS MODELLING FOR DISTORTIONS IN MANUFACTURING OF POLYMER COMPOSITE MATERIALS

K. Çınar[1*], N. B. Ersoy[1], F.E. Öz[2]

[1]*Mechanical Engineering Department, Bogazici University, TR-34342 Bebek, Istanbul, TURKEY*
[2]*Mechanical Engineering Department, Yildiz Technical University, TR-34349 Yildiz, Istanbul, TURKEY*
**kenan.cinar@boun.edu.tr*

Keywords: Polymer-matrix composites, Residual/internal stress, Finite element analysis

Abstract

A 3D Finite Element model has been developed for predicting shape distortions during curing of fibre reinforced composite parts. The total curing process is divided into three steps that corresponds the states that resin is passing through during curing: viscous, rubbery, and glassy. The material property changes during curing are implemented in the model through a three step user subroutine. Composite parts of various geometries (U-section and L-section laminates), stacking sequences, and thicknesses are manufactured. These parts were scanned using a 3D laser coordinate scanner to obtain the geometry of the distorted parts. Results show that a simple two dimensional analysis is not sufficient to capture the complex distortion patterns. Spring-in values are not constant along the length of the parts. A 3D model is proposed to capture the real distortion patterns of complex shapes.

1. Introduction

The final shape of the parts made of composite materials is not same as the mould shape after the manufacturing process. The solution of this problem is very complex because the absolute magnitude of the distortion is difficult to predict and is often show a large variation even if the manufacturing conditions are held constant. Over the years, several studies have been performed to understand the mechanisms behind these distortions [1-4], and to develop models that predict these distortions [5-8]. Most of the models take into account the effects of thermal expansion anisotropy, cure shrinkage and tooling constraints as a contributor for process induced distortions. The contributing factors to spring-in is classified as reversible (anisotropy of thermal expansion coefficient) and irreversible (cure shrinkage, material property gradients, and stress gradients due to tool-part interaction) by temperature. One of the pioneering attempts to predict spring-in in corner sections is done by Johnston *et al*. [5] who developed a plane strain finite element model which employs a cure hardening, instantaneous linear elastic constitutive model to predict process-induced stress and distortion of composite laminates. They analysed the effect of thermal expansion, cure shrinkage, temperature gradients, degree of cure, resin flow and tool-part interaction on deformation of the laminates. The tool-part interaction was modelled by elastic "shear layer", which performed until the tool is removed. In their study Svanberg and Holmberg [7] developed a simplified mechanical constitutive model to predict the shape distortions. They assumed that the mechanical behaviour of the material is constant within each material phase and there is a

step change in the properties at the glass transition temperature. They used three different tool-part interaction models in their FE analysis; freestanding, fully constrained, and frictionless contact conditions. The predictions indicated that the contact boundary conditions give closest agreement to the measured spring–in. Then they used their finite element model to predict the spring-in in brackets produced by Resin Transfer Moulding.

In most studies to date to predict the spring-in at corner sections, a 2D plane strain model is used and the spring-in is assumed to be constant along the length of the part. In this study, it was shown that 2D models cannot capture the distortions along the length direction of the composite parts, whereas a 3D model is only capable of capturing the full deformation pattern. The 2D and 3D models in the present study are extensions of the previously developed three step model [8].

2. Experimental work

2.1. Material and fabrication

The autoclave equipment consists of a U-shaped steel tooling of hot work tool steel. By closing the open sides of the tool, a mini autoclave is formed. Heat is applied around the U-shaped tool with plate heaters and pressure is applied through the compression and the vacuum ports. The shape and dimensions of the mini autoclave are shown in Figure 1. The temperature is controlled with a three channel PID controller. The uniformity of the temperature around the surface of the U-section tool is checked by 8 thermocouples.

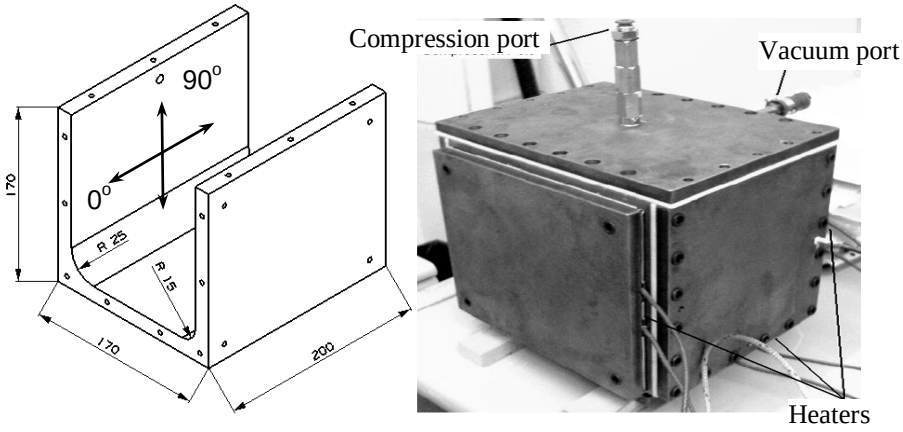

Figure 1. The mould used in manufacturing: (a) dimensions in mm. (b) closed to form an autoclave

All specimens in this work were manufactured by hand cutting and hand lay-up of the carbon-epoxy prepreg material. The material used was AS4/8552 unidirectional tape with a nominal thickness of 0.184 mm and a fibre volume fraction of 57%. In order to allow easy removal of composite parts from tool, a glass fiber reinforced PTFE release film with a nominal thickness of 80 μm was applied on the tool surface. For fabricating L-section laminates only one side of the tool was used. For U shaped laminates prepregs were laid on both sides. The schematic drawing of the process is shown in Figure 2.

The Manufacturer's Recommended Cure Cycle (MRCC) includes five steps. In the first step, the part is heated up to 120°C at 2°C/min. In the second step, it is held at 120°C for 60 minutes. In the following step, it is heated up from 120°C to 180°C at 2°C/min. Then, the part

is held at 180°C for 120 minutes. Finally, the part is left to cool down to room temperature before removal from the mould. 0.7 MPa pressure is applied from the beginning to the end of the process and vacuum is applied up to the middle of the second step.

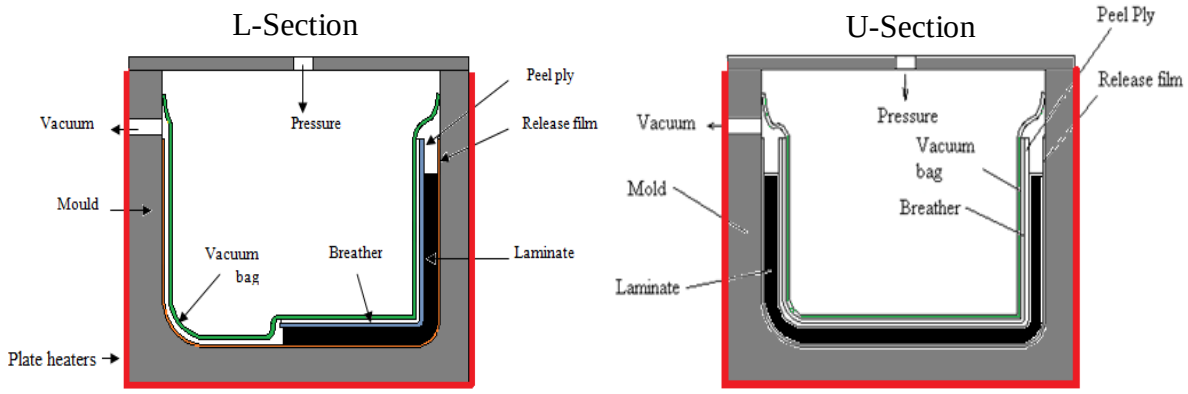

Figure 2. Schematic representation of specimen manufacturing.

2.2. Measurement of part geometry

The manufactured parts are scanned by METRIS MCA II 7-axis laser scanner in order to capture full deformation pattern of the parts. The scan data then are processed through RAPIDFORM XOV package program. Scanned geometry of the part is virtually placed on the nominal tool through three edge point and the gap distances between the tool and the part are obtained.

3. Finite element analysis (FEA)

A 3D-three step model is developed for predicting the distortions through processing. In the model, the mechanical properties are assumed to be constant within each material phase; viscous, rubbery, glassy, and the mechanical properties of a single lamina are assumed to be transversely isotropic. The first step of the model (Step-1) includes viscous state properties of the composite. It is difficult to measure the properties in this step and there are no data in the literature relating to viscous behaviour. The properties used in this step are assumed to be linear elastic and taken from optimization analysis [9] and shown in Table 1. In Step-2, rubbery mechanical properties calculated previously by micromechanics [8] are used. Due to cross-linking reactions, contraction occurs through the thickness direction in the rubbery step.

To obtain the experimentally measured 0.48% transverse cure shrinkage in this step, an equivalent negative coefficient of thermal contraction is used as given in Table 1. In Step-3 of the model, the properties of the material are switched to glassy properties. The CTE value given in this table for glassy state is the nominal value, and actual values are calculated as a function of corner thickness [9]. In Step-1 and Step-2, an autoclave pressure of 0.7 MPa is applied on the surfaces at the bag side of the part. In Step-3, the applied pressure is deactivated, the part is separated from the tool and deformations develop. In all three steps uniform temperature is assigned to the parts because the temperature range measured across the thickness and in the plane of the part at eight stations is within a 3°C band for even the thickest (16 plies) laminates. The change of material properties from one step to the next is implemented in the analysis by means of a user subroutine UMAT, which updates the elastic properties at the beginning of each step, and the stresses locked-in at each step are added up to find the final stress state after removal from the mould. Interaction between the tool and the

part is modelled by using ABAQUS mechanical contact interaction modelling capabilities [10].

Property	Unit	Viscous	Rubbery	Glassy
E_{11}	MPa	132200	132200	135000
$E_{22} = E_{33}$	MPa	80.0	165	9500
$G_{12} = G_{13}$	MPa	20.0	44.3	4900
G_{23}	MPa	20.0	41.6	4900
$\nu_{12} = \nu_{13}$	-	0.346	0.346	0.3
ν_{23}	-	0.982	0.982	0.45
α_{11}	με/°C	-	-	0
$\alpha_{22} = \alpha_{33}$	με/°C	-	-31.7	32.6
ε_{11}^{cure}	%	-	0	-
$\varepsilon_{22}^{cure} = \varepsilon_{33}^{cure}$	%	-	0.48	-

Table 1. Material properties in the viscous, rubbery and the glassy state.

Tool-part interaction was implemented to the model through classical isotropic Coulomb friction model in the tangential direction and "hard" contact relationship in the normal direction. Coulomb friction model includes two parameters; the limiting sliding stress, τ_{max} and the proportionality constant, μ. Up to limiting sliding stress, pressure is proportional to the interfacial shear stress. When the interfacial shear stress exceeds the limiting stress, sliding occurs. In the first and the second step of the analysis, tool-part interaction is active and in the third step tool-part contact is deactivated. Following the findings of Garstka et al. [11], the sliding stress τ_{max} is changed from 0.1 MPa to 0.2 MPa in the second step because the friction behaviours of these two steps (viscous and rubbery) are different. Frictional properties (τ_{max}, μ) were assumed to be isotropic for 3D model. The 2D L-section composite parts of 100 mm arm length and 15 and 25 mm corner radius were modelled together with the female steel tool, as shown in Figure 3. Only half of the part is modelled by taking advantage of the symmetry condition. The elements used in the 2D and 3D model are 8-node biquadratic quadrilateral generalized plane strain elements (CPEG8R) with reduced integration and 8 node linear brick elements (C3D8) respectively. Each ply has one element through thickness for both models. The sliding boundary conditions on the flat upper side of the tool enable the tool to expand or contract along the longitudinal direction but prevent free body motion of the tool. On the symmetry line, symmetry boundary conditions are used. L-section parts are modelled with only a quarter of the full part, since there are two symmetry planes, whereas U-sections are modelled with half of the full part as can be seen in Figure 4. Autoclave pressure is applied as a surface pressure. The tool can extend or contract freely. U-section parts also have sliding boundary conditions at the bottom side of the tool. Symmetry boundary conditions and applied pressure for 3D model can be seen in Figure 4.

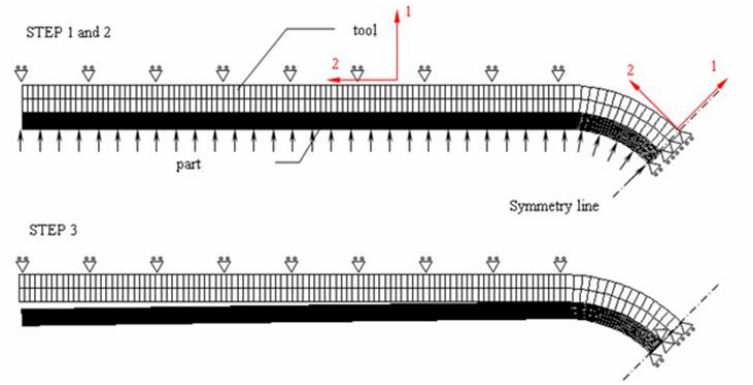

Figure 3. The finite element mesh and boundary conditions for 2D model.

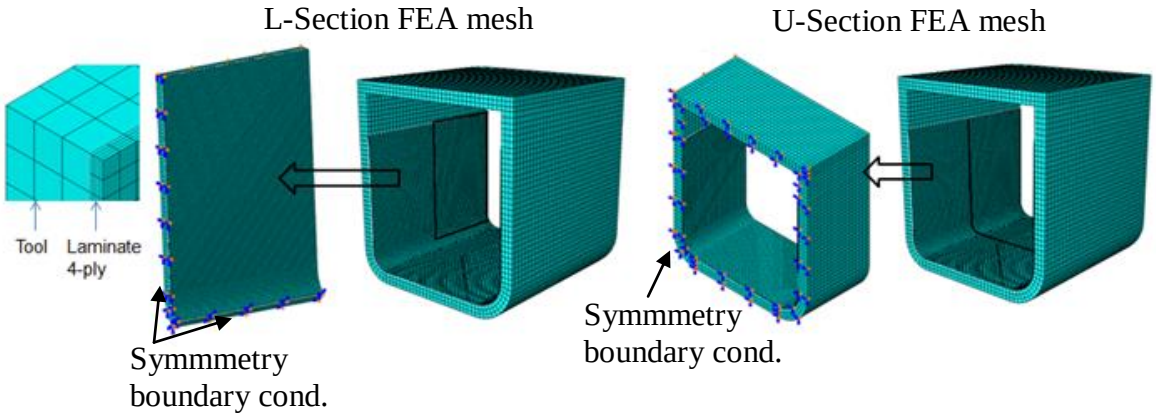

Figure 4. The finite element mesh and boundary conditions of L and C section parts for 3D model.

4. Results and discussion

2D models are not sufficiently capable of modelling of complex composite parts, because in the third direction (length direction) mechanisms such as tool-part interaction, and cure shrinkage affect the deformation causin complex deformation patterns. As shown in Figures 5 and 6, the 2-D models for both cross-ply (XP) parts and unidirectional (UD) parts predicts close values at the mid-sections, however, the predictions deviates from measurements in the edge sections. Therefore it is inevitable to use 3D models for modelling of complex composite parts.

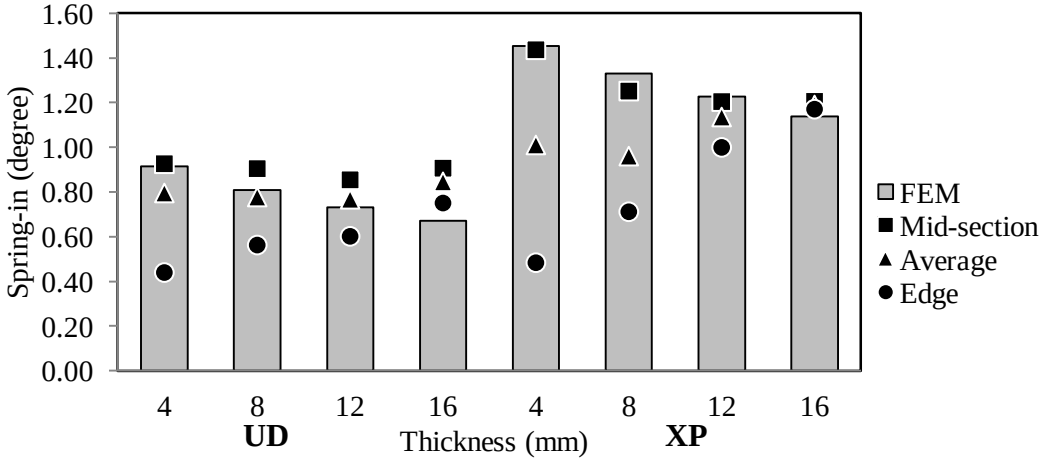

Figure 5. Spring-in values for R15 L-section laminates; 2D FEA predictions versus measured values.

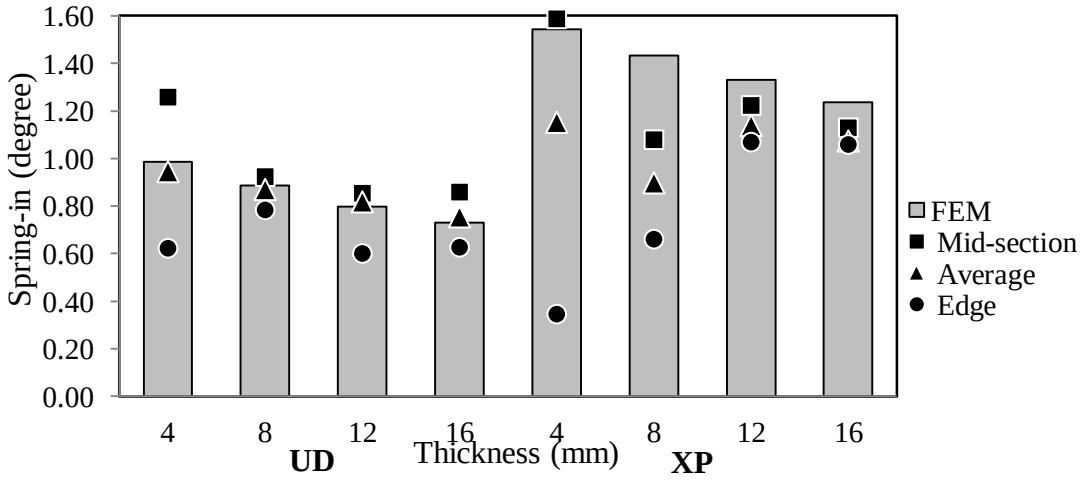

Figure 6. Spring-in values for R25 L section laminates; 2D FEA predictions versus measured values.

Tool-part interaction in the length direction causes the part to warp and results in non-constant spring-in value along this direction. Figure 7 and 8 shows the deformation patterns of L- and U-shaped parts obtained by laser coordinate scanning. As seen in the Figure 7, the distortion at the mid sections is larger than edges of the laminate. It is also observed that the warpage along the length direction is higher for cross-ply (XP) parts as compared to unidirectional (UD) parts. The reason behind this observation is the fact that in the unidirectional parts there are no fibres along length direction so that the expansion of the part in that direction is not constrained resulting in less residual stress and warpage. On the other hand, the fibres along length direction in the cross-ply parts prevent free expansion of the part possibly resulting in higher tool part interaction stresses and higher residual stresses and warpage. Same deformation patterns can be seen for U-section composite laminates as shown in Figure 8.

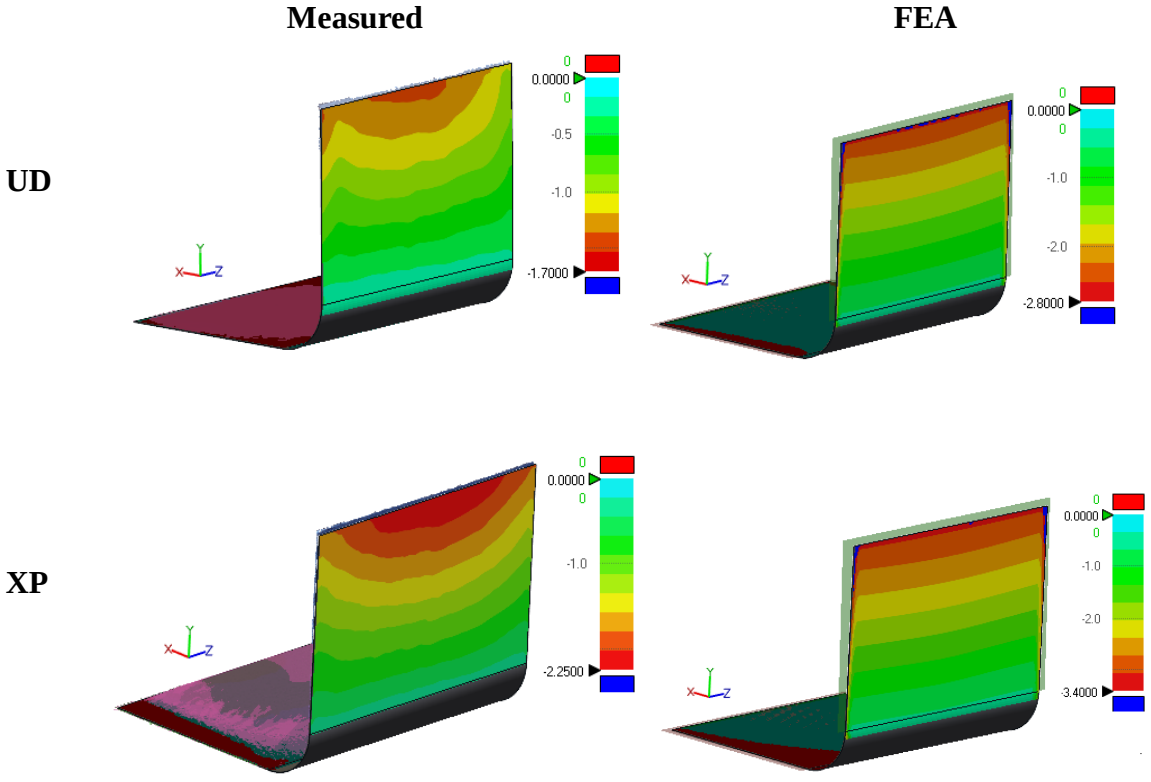

Figure 7. Deformation patterns of 4 ply L-section laminates (R25 side) (scale in mm)

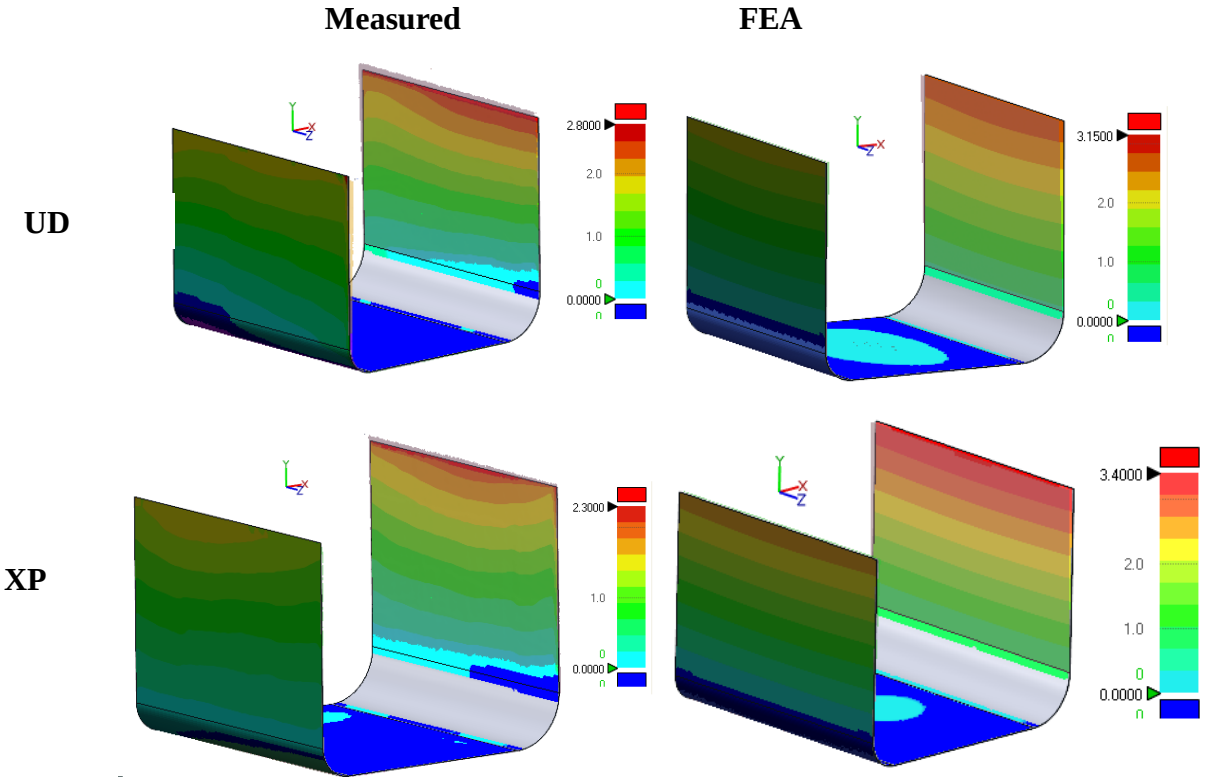

Figure 8. Deformation patterns of 4 plies U-section laminates (scale in mm)

The 3D model developed captured this deformation pattern quite well but the magnitude of the deformation was over-predicted. As the thickness of the laminate decreases the tool part interaction is to be more effective. Using this phenomenon, the tool-part interaction properties can be calibrated by comparing 3D FEA results and measured values for single ply lamina. Single ply lamina gives spring-out as represented in Figure 9. A combination of tool-part interaction parameters (friction coefficient and sliding shear stress) and mechanical properties in the viscous and rubbery states that will give the observed deformation pattern will be sought by a parameter optimization process and then used in thicker sections in the future work.

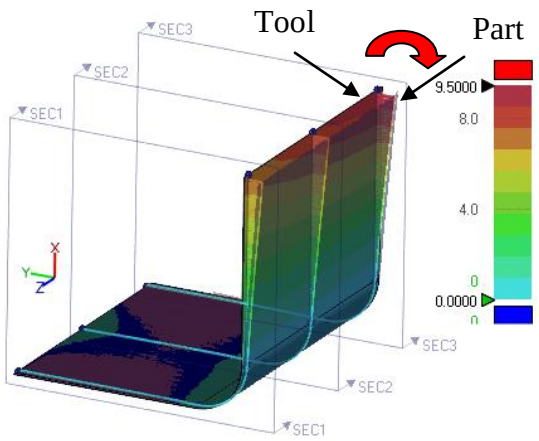

Figure 9. Spring-out in single ply part (scale in mm).

5. Conclusions

For L- and C- section parts spring-in values are not constant along the length direction. The spring-in values at the mid-section of the parts is higher than edge of the parts. It was thought that the warpage along length direction due to tool-part interaction change spring-in value along the length direction. 2D models do not have capability of predicting deformations for complex shaped parts so that 3D models should be used. 3D FE model can be calibrated for tool-part interaction parameters using a single ply part showing spring-out.

6. Acknowledgements

Authors would like to thank Boğaziçi University Research Fund for the financial support provided under Grant 09A601P

References

[1] Radford D.W., Rennick T., Separating sources of manufacturing distortion in laminated composites. J Reinforced Plast Compos 2000;19(8):621–41.
[2] Darrow DA Jr, Smith, LV. Isolating components of processing induced warpage in laminated composites, J Compos Mater 2002; 36(21): 2407-2419.
[3] Wisnom M.R., Gigliotti M., Ersoy N., Campbell M., Potter K.D., Mechanisms generating residual stresses and distortion during manufacture of polymer–matrix composite structures. Compos Part A-Appl S, 2006;37:522–529
[4] Fernlund G, Rahman N, Courdji R, Bresslauer M, Poursartip A, Willden K, Nelson K. Experimental and numerical study of the effect of cure cycle, tool surface, aspect ratio, and the lay-up on the dimensional stability of autoclave-processed composite parts. Compos Part A-Appl S 2002;33:341–51.
[5] Johnston A., Vaziri R., Poursartip A., A plane strain model for process induced deformation of laminated composite structures. J Compos Mater 2001;35(16):1435–69.
[6] Zhu Q, Geubelle, PH, Li M, Tucker CL III. Dimensional accuracy of thermoset composites: simulation of process-induced residual stresses. J Compos Mater 2001; 35(24): 2171-2205.
[7] Svanberg, J., M., and Holmberg, J., A., "Prediction of Shape Distortions. Part II. Experimental Validation and Analysis of Boundary Conditions", Compos Part A-Appl S 2004; 35: 723-734
[8] Ersoy N, Garstka T, Potter K et al. Modelling of the spring-in phenomenon in curved parts made of a thermosetting composite, Compos Part A-Appl S 2010;41: 410-418
[9] Çınar K, Ozturk U., E., Ersoy N., Wisnom M. R., Modelling manufacturing deformations in corner sections made of composite materials, submitted to Composites A
[10] ABAQUS Online Documentation, Version 6.9-1; Hibbit, Karlson, and Sorensen Inc. 2004.
[11] Garstka T., Ersoy N., Potter K., Wisnom M. R., Observations of tool-part interaction in curved composite laminates, submitted to Composites A